The Application of Laser Welding in the Processing of Aluminum Alloy Supports for Ships

Lu Xuan, Zhang Sen, Han Zhaocheng
Shandong University of Aeronautics, Binzhou, China

Corresponding Author: Lu Xuan

Abstract. Based on laser welding technology, weld samples of steel and aluminum alloy joints for marine support parts were prepared. Parameter design and joint cleaning were carried out before welding. In order to ensure the effective connection of the weld, the swing laser welding was used, and the laser power should be slightly increased when compared with the traditional welding method. Seven different samples were obtained under different process parameters, and their macro morphology, microstructure and hardness were measured and analyzed. The results show that the grain direction of the joint heat affected zone is different. These randomly distributed grains can improve the mechanical properties of the welded joint, because the force exerted on the welded joint will be evenly distributed inside the needle grain, thereby reducing the strain inside the grain and near the grain boundary, slowing the stress concentration, and making the surface of the material stressed evenly. When the laser scans the surface of the material, with the extension of the laser scanning time, the heat accumulation of the laser on the plate increases, and there is more energy in the joint to support the grain growth in the weld. The content of brittle intermetallic compounds in weld is decreased with the decrease of weld penetration. The joint action of mechanical connection and metallurgical connection is beneficial to improve the shear strength of welded joint.

Keywords: laser welding, metal forming, microstructure, hardness, mechanical property

I. Introduction

With the increasing demand for ship transportation, lightweight research has become one of the important development directions [1]. At present, many countries use aluminum steel composite building structures in the manufacturing of ships, which means using aluminum alloy to replace the original steel superstructure of fishing boats. Due to the higher density and weight of steel compared to aluminum alloys, steel aluminum structures can reduce the weight of the ship's hull, improve its navigation speed and carrying capacity [2, 3]. At the same time, the center of gravity of fishing vessels with steel aluminum structure is lower than that of fully steel structure fishing vessels. The state of being light on top and heavy on bottom is conducive to improving the stability of fishing vessels, reducing their weight, improving their carrying capacity, reducing fuel consumption, and improving navigation speed [4]. This directly improves the transportation efficiency of fishing vessels and promotes the economic development of agriculture and fisheries. However, welding between different materials is prone to defects or insufficient strength [5]. In order to solve this problem, laser welding method was proposed to be applied in the steel aluminum welding process of ship support components in the paper. Laser welding, as a welding technology, has advantages such as energy concentration, high utilization rate, and low residual stress, and is often used in the welding of dissimilar materials. The advantage of utilizing the technology of new welding processes to precisely control the heat input between interfaces effectively controls the formation of brittle phases in intermetallic compounds, increases welding practicality, and improves the service life of fishing vessels.

II. Design of welding process parameters and test plan

2.1 Weld Preparation and equipment

The experimental materials include 5083 aluminum alloy with a thickness of 1mm commonly used in fishing boats and DP780 duplex stainless steel with a thickness of 1.2mm. The plate size used for laser spot welding is 20mm × 80mm, the plate size used for laser lap welding is 100mm × 180mm. Before welding, use a steel brush to polish the surface of the plate, remove the oxide layer on the surface, and then clean the steel plate and aluminum plate with ethanol to remove surface impurities and grease. The experimental setup for laser welding is shown in Fig.1. The laser adopts Trumpchi Truss 10002 disc laser, the maximum output power is 10 kW, and the minimum core diameter is 200 μm. The laser wavelength is 1030nm, the power output stability is ±1% at rated power, and it operates continuously. The welding joint adopts Trumpf PFO3D, with a joint size of 12mm × 266mm × 366mm, weighing 35kg, this connector can achieve continuous waves, with a maximum power limit of 8000W, a collimator of 138mm, and a maximum focal length of 900mm. The laser cable type is LLK-D. The robot used in the experiment is a 6-axis KUKA load robot with a maximum load capacity of 100kg, a working area of 2800mm, and an accuracy of ± 0.04mm.

(a) laser structure (b) six degree of freedom robotic arm

Fig.1 The main equipment for laser welding

2.2 Parameter setting and adjustment

This experiment used multiple different scanning paths, and the specific path diagrams. The welding schematic diagram of the steel aluminum joint is shown in Fig.2, using the overlapping method of upper steel and lower aluminum, with argon gas as the protective gas, and a flow rate of 15 L/min. Compared with traditional welding modes, when using swing laser welding, it is necessary to slightly increase the laser power to ensure effective connection of the weld seam. Due to different swing modes, the energy of the laser energy acting on the surface of the substrate will also change. In the conventional welding process, the scanning path is a straight line, and the accumulation of heat increases with the increase of welding time. When swinging welding, the laser will stir the molten pool during welding, which is beneficial for the heat dissipation of the molten pool. Therefore, increasing laser power during swing welding can achieve the same amount of heat input. Therefore, the essence of heat input variation is to study the effect of laser power on welding results.

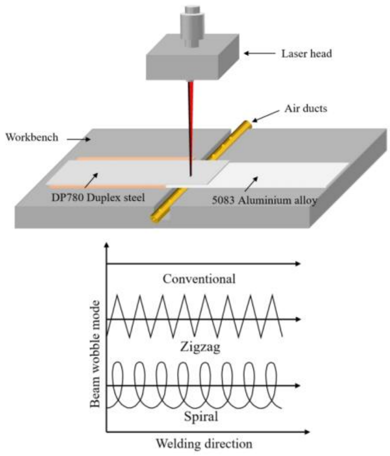

(a) Overlap welding schematic diagram
(b) Laser scanning path

Fig.2 Laser welding schematic diagram

2.3 Design of test plan

Use wire cutting to divide the metallographic specimen along the direction perpendicular to the weld seam. Clean the surface oil stains with alcohol, and use 600 #, 1000 #, 1500 #, and 2000 # metallographic sandpaper to polish the surface of the metallographic specimens in sequence. When replacing the high magnification sandpaper, rotate the grinding direction 90 °, and then use a metallographic specimen polishing machine and diamond polishing paste to mechanically polish the surface of the specimens to obtain a glossy mirror surface. Use a weak acid solution to corrode the surface of the sample, and the corrosion time is generally 6 seconds.

The mechanical performance testing equipment is shown in Fig.3, including microhardness tester and tensile testing machine. Use a micro Vickers hardness tester to measure the microhardness of welded joints, with a loading force of 500g and a holding time of 10s. Use an electronic universal tensile testing machine for tensile testing, and perform tensile testing on the processed tensile parts at room temperature. In order to ensure that the force on the lap joint remains in the same straight line during the shearing process of the specimen, 1.2mm and 1mm thick backing plates are added to the base metal on both sides to ensure that the tensile force is parallel to the joint interface.

(a) microhardness tester (b) tensile testing machine

Fig.3 Mechanical performance testing equipment

III. Effects on weld joints and microstructure

3.1 Macro morphology rating analysis

Process parameters of different samples is shown in Tab.1. The macroscopic morphology of steel aluminum alloy joints under different welding modes is shown in Fig.4. It can be seen that the morphology of the weld surface can be changed by laser oscillation. The effect area of the spot on the plate changes, leading to a concentration of laser energy density. Both steel and aluminum plates melt through. The surface of the weld seam is dark gray, and the weld seam welded by both paths has a relatively rough surface. The top and root of the weld seam show obvious concavity and convexity, with some uneven transitions. When using other scanning paths for welding, the contact area between the laser and the plate changes, and at this time, the surface of the base material is uniformly heated, and there is no weld penetration. During swing welding, the variation of the swing pattern has a significant impact on the spot welding joint. Relatively speaking, the forming effect of welding joints 1 #, 2 #, 3 #, 5 #, and 7 # is better, and there is no smooth transition at the top and bottom.

Table.1 Process parameters of different samples

Number	Power /W	Input energy/E	Swing width/ mm	Swing period/ mm	Swing frequency/Hz
1	1650	750.47	1.2	1	20
2	1600	750.47	1.2	1	20
3	1550	706.91	1.2	1	20
4	1550	706.91	1.2	0.925	20
5	1400	706.91	1.2	0.925	20
6	1450	686.84	1.2	0.925	20
7	1350	599.89	0	0	0

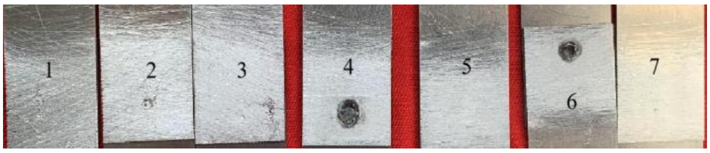

Fig.4 Weld morphology of different spot welded joints

There are obvious welding marks on the back, and cracks appear at the top of the joint that run through the entire joint. When a large tensile force is applied or a large pressure is applied at the top, it is easy to cause welding failure, and the mechanical properties of the welded joint are poor. The density of the laser power acting on the surface and inside of the material decreases, and there are a small number of spots on the back of the welded joint. In the scanning path, welding joints all produce varying degrees of defects, such as collapse, cracks, pores, etc. The main reason is that during the welding process, the erosion of elements such as zinc and magnesium can easily cause keyhole collapse and metal overflow. The generation of pores has a negative impact on the performance of the joint, but the presence of zinc is essential as it can ensure the wettability of molten aluminum on the steel surface. Due to a small number of welding defects, the actual demand is not significantly affected. Due to changes in the scanning path of the laser beam, the size of the spot welded joint also changes. The dimensions of steel aluminum alloy joints using different welding modes are shown in

Fig.5. The laser is constantly in a swinging state, and the contact area between the laser and the base material increases, while the energy decreases. The aspect ratio of the weld seam during swing welding is smaller than that of conventional welding. From this, it can be seen that when parameters such as welding speed and laser power are constant, the change in laser swing mode will change the energy density of the surface spot of the workpiece, thereby affecting the stability of welding and the formation of the weld seam. The laser scanning path to some extent determines the depth to width ratio of the weld seam.

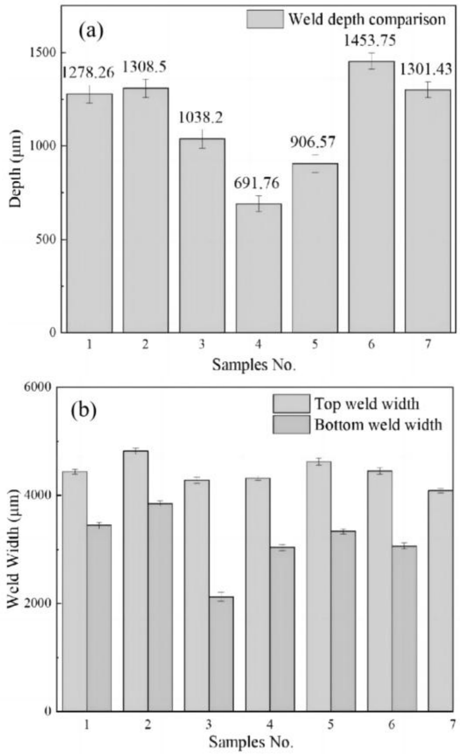

Fig.5 Weld size of different specimens

3.2 Analysis of metallographic structure

The steel aluminum welding joint mainly consists of three parts: fusion line, heat affected zone, and weld seam. Because the metallographic structure of the heat affected zone of the seven types of welded joints is the same, all of which are composed of tempered ferrite and block ferrite, and the grain size gradually transitions from small to large to the weld zone. So we only compare the differences in the metallographic structure of the fusion line, weld top, and weld bottom of the seven types of welding joints, and analyze the influence of different scanning paths on the metallographic structure of the welding joints. The metallographic structure of the fusion line area of different steel aluminum joints is shown in Fig.6. The metallographic structure of joints 1 #, 3 # and 5 # is similar, and the fusion line is composed of a large amount of martensite and ferrite. At the bottom of the weld seam is ferrite, with a small amount of sheet-like pearlite at the bottom of joints 1 # and 3 #. The fusion line of joints 2 #, 4 #, and 6 # is mainly composed of two components: ferrite and martensite. The bottom of the weld seam is entirely composed of ferrite. The grain direction in the heat affected zone of the joint is different. These randomly distributed grains can improve the mechanical properties of welded joints, as the force applied to the welded joint will be uniformly distributed inside the needle shaped grains, reducing strain forces inside the grains and near grain boundaries, slowing down stress concentration, and making the material surface uniformly stressed.

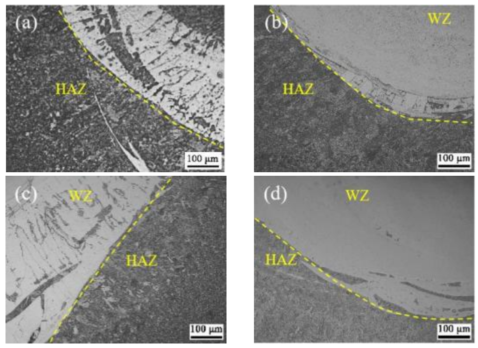

(a) 1# (b) 2# (c) 3#
(d) 4#

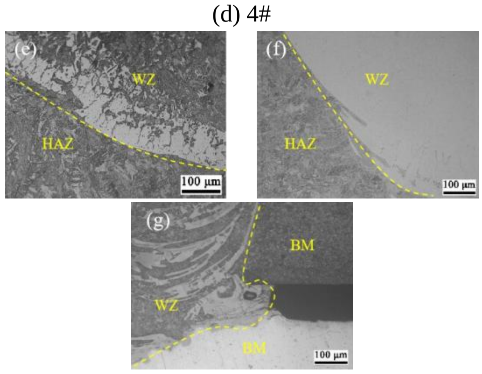

(e) 5# (f) 6# (g) 7#

Fig.6 Bottom structure of different welded joints

IV. Analysis of mechanical properties

4.1 Testing of hardness characteristics

The microhardness load variation of steel side welded joints under different welding parameters is shown in Fig.7. It can be seen that the maximum microhardness of the 5 # steel side joint is 450HV, while the maximum microhardness of the conventional welded steel side joint is 424HV. The maximum microhardness of swing welded steel/aluminum joints has been improved. However, the average microhardness of the swing welding seam area is lower than that of conventional welding. When swinging welding, when the laser scans the surface of the material, as the laser scanning time prolongs, the heat accumulation of the laser on the plate increases, and there is more energy in the joint to support the grain growth in the weld. Therefore, the grain size is larger, resulting in a much higher ferrite content in the weld than martensite. Therefore, the average microhardness of the weld seam area in swing welding is slightly lower. The content of martensite in the weld seam of conventional welding joints is relatively high, while the content of ferrite is low. The microstructure grains show irregular dispersion, which is conducive to the dispersion of force after being subjected to force. The force applied to the surface will be evenly distributed on the material surface to prevent stress concentration. Whether it is swing welding or conventional welding, the heat affected zone of the weld seam is the highest value of microhardness.

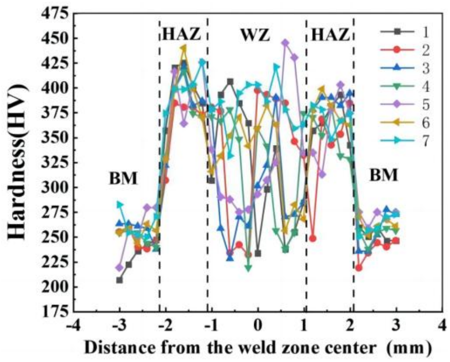

Fig.7 Microhardness of welded joints under different scanning paths

4.2 Testing of strength characteristics

The tensile load changes of the steel aluminum welded joints obtained under different process parameters are shown in Fig.8. It can be observed that compared to conventional welding, the performance of the joints in swing welding is improved, with a maximum shear strength of 83N/mm. When using conventional welding, the shear strength of the steel/aluminum joint is 39N/mm. When swinging welding, the laser scanning material surface increases, the energy received by the weld unit decreases, and the connection area of the steel aluminum joint increases. The weld penetration depth is shallow, and the steel/aluminum joint surface is poor. When the swinging amplitude increases, the width of the steel/aluminum joint surface increases, and the effective bearing area increases. The decrease in penetration depth of the joint reduces the generation of brittle intermetallic compounds in the weld, and the applied force can be better dispersed, which helps to improve the shear strength of the weld. During conventional welding, the penetration depth of the joint increases, which means that the steel aluminum reaction is enhanced. Therefore, the content of brittle intermetallic compounds in the weld increases. A large amount of brittle intermetallic compounds will affect the mechanical properties of the weld, and fracture will be more likely to occur at the steel aluminum connection. In addition, the decrease in weld penetration reduces the content of brittle intermetallic compounds in the weld. The combined effect of mechanical and metallurgical connections is beneficial for improving the shear strength of welded joints.

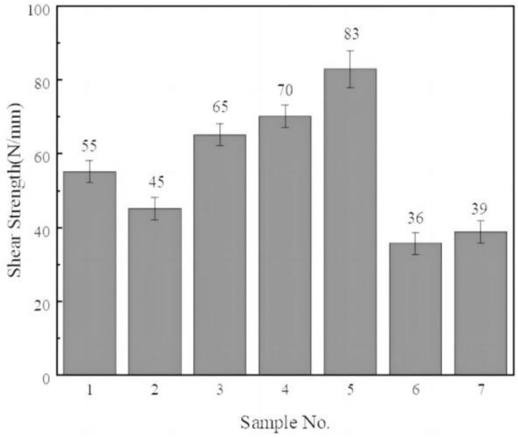

Fig.8 Shear strength of joints with different scanning paths

V. Conclusions

The improvement of welding performance of steel and aluminum plays an important role in promoting the lightweight of marine supports. Different scanning paths were applied to dissimilar joints of steel and aluminum alloys, and based on experimental testing, mechanical performance comparison results were obtained under laser welding process parameters. The results indicate that when using the parameters of specimens 4 and 6 for corresponding scanning paths in welded steel aluminum welding, the energy of the light spot acting on the surface of the workpiece has a large proportion to the heat input of the welding pool and the energy density of the material surface, resulting in poor forming effect of the sheet metal. It can be proven that changes in the scanning path directly alter the energy distribution of the laser on the surface of the workpiece. During swing spot welding, the temperature of the molten pool is uniform throughout, and the grains are mainly composed of a single martensite. During non swing welding, as the depth of fusion increases, the laser energy gradually decreases and the grains are mainly ferrite. In the shear strength test, except for the joint of specimen 6, the shear strength of all other joints was better than that of specimen 7 without swing welding. The mechanical properties of the joint obtained using the scanning path of sample 5 were the best. Compared to non swing spot welding, the microhardness was increased by 1.06 times and the shear strength was increased by 2.12 times.

Acknowledgement

The paper was support by National College Student Innovation and Entrepreneurship Project (S202310449262).

References

[1.] Bing D ,Qichang L ,Changqi Z. “Application of Lightweight Structure in Automobile Bumper Beam: A Review”. *Materials* 16. (2023). DOI: 10.3390/MA16030967

[2.] Stefan R ,Nowfal H A ,Volker V. “High-Speed Laser Beam Welding of Magnesium Alloy AZ31 for Enhancing the Mechanical Properties”. *Key Engineering Materials*, 7025.(2023). DOI:10.4028/P-J28RCR

[3.] Didi Faouzi. “Probing the impact of process variables in laser-welded aluminum alloys: A machine learning study”. *Materials Today Communications* 38.(2024). DOI:10.1016/J.MTCOMM. 2023.107660

[4.] Lina SunYou Lu,and Junxiang Jiang. “Effect of laser welding and laser wire filling on forming and properties of dissimilar steel welded joints”. *Materials Research Express* 10.12(2023). DOI:10.1088/2053-1591/AD0DD1

[5.] Wang Shuwen. “Crystallographic characteristics and mechanical behavior of laser welded joints of hot roll bending parts”. *Materials Characterization* 207.(2024). DOI:10.1016/J.MATCHAR. 2023.113466